Modeling Electron Transfer in Biochemistry: A Quantum Chemical Study of Charge Separation in *Rhodobacter sphaeroides* and Photosystem II

Margareta R. A. Blomberg,*,† Per E. M. Siegbahn,† and Gerald T. Babcock‡

Contribution from the Department of Physics, Stockholm University, Box 6730, S-113 85 Stockholm, Sweden, and Department of Chemistry, Michigan State University, East Lansing, Michigan 48824

Received February 17, 1998. Revised Manuscript Received June 8, 1998

Abstract: High-level quantum chemical methods (hybrid density-functional type) are applied to the light-driven charge-separation process in the photosynthetic reaction centers of both bacteria and photosystem II in green plants. Structural information on the bacterial system provides the basis for choosing the models used in the calculations. The energetics of the electron transfer from the (bacterio)chlorophyll to the quinone are calculated as well as those of the intermediate step involving the (bacterio)pheophytin. The surrounding protein is treated as a dielectric medium, and the cavities around the solute molecules are determined by isodensity surfaces. The dielectric effects on the charge-separation processes are calculated to be as large as 50 kcal/mol. It is shown that hydrogen bonding between the chromophores and certain peptide residues as well as the axial histidine ligand on the (bacterio)chlorophylls contributes substantially to the energetics. Good agreement with experimentally estimated driving forces of the different steps is obtained within 2 kcal/mol for the bacteriosystem and within 8 kcal/mol for photosystem II. The results for photosystem II have a lower accuracy, as expected, due to the lack of detailed structural information on this system. Recent low-resolution data indicating a weaker coupling between the chlorophylls in P680 as compared to that of the special pair in the bacterial systems are taken into account in the calculations. In the bacterial system, charge separation to the accessory bacteriochlorophyll is essentially thermoneutral and the $P865^+BPheo^-$ state is stable by 7.5 kcal/mol. In photosystem II, charge separation to the $P680^+Pheo^-$ state is much less strongly driven, and the absence of an axial histidine ligand to the accessory chlorophyll appears necessary to allow its formation. The creation of the tyrosine radical (Y_Z) by proton-coupled electron transfer to the photoionized reaction center chlorophyll in photosystem II is also studied. In this case as well, hydrogen bonding to other peptide residues plays an important role in the overall energetic balance of the reaction.

I. Introduction

The fundamental photochemical process in photosynthesis involves the light-driven separation of charge in the low-dielectric-constant environment of the reaction center polypeptide complex. Ultimately, the photochemistry produces a one-electron reduced quinone species and a one-electron oxidized reaction center (bacterio)chlorophyll complex. In the reaction centers of photosynthetic bacteria and in photosystem II (PSII) in algae and plants, the fates of the separated electron and hole differ. In bacteria, the electron on the semiquinone (Q_A^-) recombines with the hole on the bacteriochlorophyll complex ($P865^+$ in *Rhodobacter (Rb.) sphaeroides*) through the intermediacy of the cytochrome bc_1 complex. The recombination process is linked to proton translocation and, ultimately, to ATP formation, which provides the energy source for bacterial growth and reproduction. In PSII, the reduced quinone (Q_A^-) transfers its electron through the cytochrome b_6f complex and photosystem I to generate the NADPH and ATP that are used in CO_2 fixation; the oxidized PSII reaction center chlorophyll complex, $P680^+$, that is produced by the photochemistry is used to oxidize water to dioxygen (for recent reviews of PSII and bacterial reaction centers see refs 1−4).

Despite the differences in the fates of the separated electrons and holes in the plant PSII and bacterial systems, there are strong structural and functional similarities between the two that have been noted for some time.[5,6] These similarities have been highlighted recently by 8 Å resolution electron diffraction data of PSII in comparison with the crystal structure of the bRC.[7] These include amino acid sequence analogies between the core polypeptides, L and M in bacteria and D1 and D2 in PSII, that comprise the core of the reaction centers, the occurrence of conserved histidines that are positioned to coordinate the chlorophylls of P680 and the bacteriochlorophylls of P865, sequence homologies in the quinone acceptor region, and the

† Stockholm University.
‡ Michigan State University.

(1) Ort, D. R., Yocum, C. F., Eds. *Oxygenic Photosynthesis: The Light Reactions*; Kluwer: Dordrecht, The Netherlands, 1996. Witt, H. T. *Ber. Bunsen-Ges. Phys. Chem.* **1996**, *10D*, 1923.
(2) Tommos, C.; Babcock, G. T. *Acc. Chem. Res.* **1998**, *31*, 18.
(3) Deisenhofer, J., Norris, J. R., Eds. *The Photosynthetic Reaction Center*; Academic Press: San Diego, CA, 1993; Vols. 1 and 2.
(4) Michele-Beyerle, M., Ed. *Proceedings of Feldafing 3: Workshop on Reaction Centers of Photosynthetic Bacteria; Structure and Dynamics*; Springer-Verlag: Berlin, 1996.
(5) Rutherford, A. W. *Biochem. Soc. Trans.* **1986**, *14*, 15. Michel, H.; Deisenhofer, J. *Biochemistry* **1988**, *27*, 1.
(6) Diner, B. A.; Babcock, G. T. In *Oxygenic Photosynthesis: The Light Reactions*; Ort, D. R., Yocum, C. F., Eds.; Kluwer: Dordrecht, The Netherlands, 1996; p 213.
(7) Rhee, K.-H.; Morris, E. P.; Zheleva, D.; Hankamer, B.; Kühlbrandt, W.; Barber, J. *Nature* **1997**, *389*, 522.

S0002-7863(98)00526-5 CCC: $15.00
Published on Web 08/12/1998

intermediacy of a (bacterio)pheophytin acceptor preceding Q_A in the primary photochemistry.

An emerging picture suggests that there are good analogies in the primary photochemistry of the plant and bacterial systems as well but that illuminating differences exist. In both PSII and bacteria the absorption of a photon in the pigment bed produces an energy transfer that culminates in charge separation as follows: (antenna)*(k_1) $\rightleftharpoons$ (k_{-1}) (PPheo)* $\rightleftharpoons$ (k_2)(k_{-2}) (P^+Pheo^-) where the asterisk indicates an electronically excited chromophore. In the bacterial case, the P865 trap is strongly red-shifted relative to the antenna, owing to the 1300 cm^{-1} exciton coupling that occurs in the P865 bacteriochlorophyll dimer. Nonetheless, the rate constants k_1, k_{-1}, k_2, and k_{-2} are sufficiently close that exciton delocalization in the pigment bed is fast, and exciton localization to produce $P865^+BPheo^-$ results in a relatively shallowly trapped charge-separated state that relaxes on the picosecond and nanosecond time scales to produce a more stable charge separation. At 10 ns, for example, the charge-separated state is stable by about 6 kcal/mol. The subsequent charge transfer from $BPheo^-$ to Q_A generates the $P865^+Q_A^-$ state, which is stabilized by 21.7 kcal/mol relative to the initial reaction center excited state. Overall, the charge-separation process in the bacterial reaction-center preserves 11.3 kcal/mol of the 33.0 kcal/mol of excited-state energy of P865* in the $P865^+Q_A^-$ state.[3,4,6,8]

The principles that have emerged in bacteria carry over to PSII, but the overall efficiency of the charge separation is significantly greater in oxygen-evolving systems. Of the 44.0 kcal/mol of energy generated by photon absorption to produce the P680* excited state, 28.4 kcal/mol is preserved in the $P680^+Q_A^-$ charge-separated state. Recent work provides insight into the increased energy conversion efficiency in PSII. As opposed to the strong exciton coupling that occurs in the P865 dimer, exciton coupling in P680 is substantially weaker, only about 300 cm^{-1}.[6,9] This results in a much weaker spectral red shift for P680 relative to those of the other pigments in the PSII reaction center; it also leads to the spectral congestion that has complicated studies of primary photochemistry in PSII. Nonetheless, experimental data from a number of labs converge to support the view that the $P680^+$ $Pheo^-$ state is even less weakly stabilized relative to P* than is the corresponding $P865^+BPheo^-$ state and may even be slightly uphill.[8−11] As opposed to the situation in the bacterial reaction center where the excited-state population is depleted with the dominant 3 ps charge separation time,[12] the excited-state population in PSII remains substantial on the tens to hundreds of picoseconds time scale. Irreversibility becomes significant in PSII only as the $P680^+Q_A^-$ state forms; this species is stabilized by 13.6 kcal/mol relative to the P680* state. Overall, the less strongly driven formation of $P680^+Pheo^-$ and $P680^+Q_A^-$, in conjunction with the higher intrinsic ionization potential of chlorophyll compared to bacteriochlorophyll, leads to a significant increase in overall energy conversion in PSII relative to that which occurs in the bacterial case.

Although the experimental aspects of the charge-separation process in bacteria and PSII are being clarified, the underlying molecular bases for many of the observed phenomena remain obscure. The role of the local protein structure about the redox cofactors and pigments, the effects of axial ligation to the (bacterio)chlorophylls, and the effect of hydrogen bonding are not well understood, and the importance of dielectric effects, whether local or long range, is an area of considerable current activity.[13−15,2] Computational approaches have the ability to provide deep insight into these issues. However, as a result of to the complexity of the molecular structures involved and of the uncertainty, in the case of PSII, in the overall arrangement of the charge separation cofactors in the polypeptide scaffolding, these methods have only recently been applied to the bacterial system[16−18] and not at all in depth to PSII. In the work described here, we have used hybrid density-functional methods to explore the charge-separation process in both the bacterial reaction center and in PSII. Our analysis sheds considerable light on the molecular mechanisms by which charge separation is created and stabilized in photosynthesis.

II. Computational Details

The calculations were performed in three steps. First, an optimization of the geometry was performed using the B3LYP method,[19] which is a density-functional theory (DFT) type of calculation based on hybrid functionals. Double-ζ basis sets were used in this step. In the second step, the energy was evaluated for the optimized geometry taking into account the effects of diffuse functions and polarization functions. In a third step, the effects of the polarizable protein are included using a homogeneous dielectric medium. The energy evaluation and the dielectric calculations were also performed at the B3LYP level. All calculations were made using the Gaussian 94 program,[20] where for some of the dielectric test calculations the version modified by Rinaldi et al.[21] was used.

The B3LYP functional can be written as[22] $FB3LYP = (1 - A)F_x^{Slater} + AF_x^{HF} + BF_x^{Becke} + CF_c^{LYP} + (1 - C)F_c^{VWN}$ where F_x^{Slater} is the Slater exchange, F_x^{HF} is the Hartree−Fock exchange, F_x^{Becke} is the gradient part of the exchange functional of Becke,[19] F_c^{LYP} is the correlation functional of Lee, Yang, and Parr,[23] and F_c^{VWN} is the correlation functional of Vosko, Wilk, and Nusair.[24] *A*, *B*, and *C* are the coefficients determined by Becke[19] using a fit to the experimental

(8) Van Grondelle, R.; Dekker, J. P.; Gilbro, T.; Sundstrom, V. *Biochim. Biophys. Acta* **1994**, *1187*, 1.
(9) Durrant, J. R.; Klug, D. R.; Kwa, S. L. S.; Van Grondelle, R.; Porter, G.; Dekker J. P. *Proc. Natl. Acad. Sci. U.S.A.* **1995**, *92*, 4798.
(10) Gatzen, G.; Muller, M.; Griebenow, K.; Holzwarth, A. R. *J. Phys. Chem.* **1996**, *100*, 7269.
(11) Donovan, B.; Walker, L. A., II; Kaplan, D.; Bouvier, M.; Yocum, C. F.; Sension, R. J. *J. Phys. Chem. B* **1997**, *101*, 5232.
(12) Du, M.; Rosenthal, S. J.; Xie, X.; DiMagno, T. J.; Schmidt, M.; Hanson, D. K.; Schiffer, M.; Norris, J. R.; Fleming, G. R. *Proc. Natl. Acad. Sci. U.S.A.* **1992**, *89*, 8517.
(13) Creighton, S.; Hwang, J.-K.; Warshel, A.; Parson, W. W.; Norris, J. *Biochemistry* **1988**, *27*, 774. Parson, W. W.; Chu, Z. T.; Warshel, A. *Biochim. Biophys. Acta* **1990**, *1017*, 251. Alden, R. G.; Parson, W. W.; Chu, Z. T.; Warshel, A. *J. Am. Chem. Soc.* **1995**, *117*, 12284.
(14) Gunner, M. R. In *Proceedings of Feldafing 3: Workshop on the Reaction Centers of Photosynthetic Bacteria; Structure and Dynamics*; Michel-Beyerle, M.-E., Ed.; Springer-Verlag: Berlin, 1996; p 132.
(15) Steffen, M. A.; Lao, K. Q.; Boxer, S. G. *Science* **1994**, *264*, 810.
(16) Thompson, M. A.; Zerner, M. *J. Am. Chem. Soc.* **1991**, *113*, 8210. Thompson, M. A.; Zerner, M.; Fajer, J. *J. Phys. Chem.* **1991**, *95*, 5693.
(17) Warshel, A.; Parson, W. W. *J. Am. Chem. Soc.* **1987**, *109*, 6143. Parson, W. W.; Warshel, A. *J. Am. Chem. Soc.* **1987**, *109*, 6152.
(18) Scherer, P. O.; Fischer, S. F. *J. Phys. Chem.* **1989**, *93*, 1633. Scherer, P. O.; Fischer, S. F. *J. Phys. Chem.* **1992**, *96*, 574.
(19) Becke, A. D. *Phys. Rev.* **1988**, *A38*, 3098. Becke, A. D. *J. Chem. Phys.* **1993**, *98*, 1372. Becke, A. D. *J. Chem. Phys.* **1993**, *98*, 5648.
(20) Frisch, M. J.; Trucks, G. W.; Schlegel, H. B.; Gill, P. M. W.; Johnson, B. G.; Robb, M. A.; Cheeseman, J. R.; Keith, T.; Petersson, G. A.; Montgomery, J. A.; Raghavachari, K.; Al-Laham, M. A.; Zakrzewski, V. G.; Ortiz, J. V.; Foresman, J. B.; Cioslowski, J.; Stefanov, B. B.; Nanayakkara, A.; Challacombe, M.; Peng, C. Y.; Ayala, P. Y.; Chen, W.; Wong, M. W.; Andres, J. L.; Replogle, E. S.; Gomperts, R.; Martin, R. L.; Fox, D. J.; Binkley, J. S.; Defrees, D. J.; Baker, J.; Stewart, J. P.; Head-Gordon, M.; Gonzalez, C.; Pople, J. A. *Gaussian 94*, revision B.2; Gaussian Inc.: Pittsburgh, PA, 1995.
(21) Rinaldi, D.; Ruiz-Lopez, M. F.; Rivail, J.-L. *J. Chem. Phys.* **1983**, *78*, 834.
(22) Stevens, P. J.; Devlin, F. J.; Chablowski, C. F.; Frisch, M. J. *J. Phys. Chem.* **1994**, *98*, 11623.
(23) Lee, C.; Yang, W.; Parr, R. G. *Phys. Rev.* **1988**, *B37*, 785.
(24) Vosko, S. H.; Wilk, L.; Nusair, M. *Can. J. Phys.* **1980**, *58*, 1200.

heats of formation, where the correlation functionals of Perdew and Wang[25] were used instead of F_c^{VWN} and F_c^{LYP} in the expression above.

In the B3LYP geometry optimizations and dielectric calculations the LANL2DZ set of the Gaussian 94 program was used. For the magnesium atom this means that a nonrelativistic ECP, according to Hay and Wadt,[26] was used. The metal valence basis set used in connection with this ECP is essentially of double-ζ quality. The rest of the atoms are described by standard double-ζ basis sets. In the final B3LYP energy calculations ideally the large 6-311+G(2d,2p) basis set in the Gaussian 94 program should be used. This basis set has two sets of polarization functions on all atoms and also has diffuse functions. For most of the larger molecules in this study it was not possible to use this large basis set. In test calculations on quinone and chlorophyll type molecules *either* diffuse functions *or* polarization functions were added. It was found that for both ionization potentials and electron affinities of these molecules the effects of diffuse and polarization functions go in opposite directions and to a large extent cancel each other. For the smaller benzoquinone hydrogen bonded to two water molecules, the large 6-311+G(2d,2p) basis set could be applied, and the calculated electron affinity is decreased by only 0.6 kcal/mol as compared to the decrease experienced in the LANL2DZ basis set. For the chlorophyll type molecules, only one set of polarization functions could be added in the calculations, and this has a rather small effect of about 1 kcal/mol, decreasing both ionization potentials and electron affinities. Furthermore, it was not possible to include diffuse functions on all heavy atoms of the chlorophylls and the pheophytins at the same time due to linear dependence. Several test calculations were therefore done in which diffuse functions on different sets of atoms were added in each calculation. Both ionization potentials and electron affinities were found to increase slightly from these diffuse functions. It was concluded that the effects on electron affinities and ionization potentials essentially cancel each other, and therefore the LANL2DZ results are reported for both quinone type molecules and chlorophyll type molecules. In the calculations on tyrosine-containing molecules the 6-311+G(2d,2p) energies are given. In benchmark calculations on a set of smaller molecules, using the same B3LYP functional as in the present work and somewhat larger basis sets, it was shown that the average errors in ionization potentials and electron affinities compared to experimental values were 3.9 and 2.5 kcal/mol, respectively.[28] It should be noted that the type of small systems included in the benchmark test is often more difficult to treat theoretically than the larger molecules of the type included in the present study.

The dielectric effects from the surrounding protein were obtained using the self-consistent reaction field (SCRF) method.[29−32] One of the simplest models for treating long-range solvent effects is to consider the solvent as a macroscopic continuum with a dielectric constant ϵ and the solute as filling a cavity in this continuous medium. This model was introduced by Born[33] for the case of a charged species in a spherical cavity and was generalized by Kirkwood[34] leading to the well-known Onsager model[35] for a purely dipolar solute. Rivail et al.[21,27,36] have generalized this model to the case where the charge distribution of the solute is expanded in a series of multipoles, up to sixth order, and the cavity is allowed to be ellipsoidal. An ellipsoidal cavity is still not a good approximation to the shape of many molecules, and in some cases even the use of the sixth-order moment is not adequate. Tomasi has developed a polarized continuum model (PCM) that describes the solute in terms of a set of interlocking spheres having slightly enlarged van der Waals radii and calculates surface potentials for a selected number of points.[37] The solvent effect is derived from the interactions of the surface potentials with the dielectric continuum. This procedure is equivalent to going to infinite order in the electric moments. Wiberg et al.[38] have developed a modified version of this model (IPCM, isodensity polarizable continuum model) that defines the cavity in terms of a surface of constant charge density for the solute molecule. In the present study the self-consistent isodensity-polarized continuum model (SCI-PCIM) as implemented in the Gaussian 94 program[20] has been applied. In this method the solute cavity is determined self-consistently. The default isodensity value of 0.0004 e/B^3 was used, which has been found to yield volumes that are very close to the observed molar volumes. The dielectric constant of the continuum was taken to be 4. This can be considered as a parameter, effectively describing the combined effect of a protein with a dielectric constant of about 3 embedded in a water solution with a dielectric constant of 80. The electronic polarizability of many organic molecules corresponds to a dielectric constant of about 2, and if also some nuclear relaxation is allowed for, it is reasonable that a protein could be described by a dielectric constant of about 3. It can be noted that early test calculations showed that using an effective value of 3 for the dielectric constant (corresponding approximately to the value of 2 for the protein) can change the energetics for the charge separation by as much as 7 kcal/mol, while going to a larger value, $\epsilon = 5$, has a much smaller effect. These test calculations, however, were performed on the smallest model systems, which should be more sensitive to changes in ϵ than the final models actually used. The final motivation for the chosen value of the dielectric constant parameter is the good agreement with experimental energetics obtained for all three charge separation reactions in the photosynthetic bacteriosystem described below. A large number of test calculations were performed using the multipole expansion method of Rivail et al.,[21,27,36] allowing for ellipsoidal cavities in the calculations of the dielectric effects. The individual values for the dielectric effects were found to be quite different (by several kcal/mol) for the two methods. However, for the relative energies of the charge-transfer processes, the two methods gave very similar results in most cases. For example, for the smallest chlorophyll models used, discussed in section III.c, the SCI-PCM and Rivail methods gave the same results, to within about 2 kcal/mol, for both the driving force of the final charge separation leaving the electron on the quinone and the primary charge-separation step to the pheophytin. For the more elaborate chlorophyll models the ellipsoidal cavities of the Rivail method do not fit the molecular shape very well and can therefore not be used, which in particular is true when the axial histidine ligands are added.

As mentioned above, the dielectric calculations are performed at the B3LYP level. However, the calculations of the *changes* in dielectric effects from extensions of the model for the chlorophyll type molecules are performed at the Hartree−Fock level. It should be noted that the calculated dielectric effects on the *absolute* ionization potentials and electron affinities are quite similar at the B3LYP and Hartree−Fock levels, differing by 1−2 kcal/mol only. Relative effects should be even more similar.

III. Results and Discussion

The present computational study starts at the event when the reaction center (RC) of the photosystem in plants or bacteria has received the energy provided by a photon that has been absorbed by the antenna. The transfer of the absorbed light

(25) Perdew, J. P.; Wang, Y. *Phys. Rev. B* **1992**, *45*, 13244. Perdew, J. P. In *Electronic Structure of Solids*; Ziesche, P., Eischrig, H., Eds.; Akademie Verlag: Berlin, 1991. Perdew, J. P.; Chevary, J. A.; Vosko, S. H.; Jackson, K. A.; Pederson, M. R.; Singh, D. J.; Fiolhais, C. *Phys. Rev. B* **1992**, *46*, 6671.

(26) Hay, P. J.; Wadt, W. R. *J. Chem. Phys.* **1985**, *82*, 299.

(27) Rivail, J.-L.; Rinaldi, D. In *Computational Chemistry, Review of Current Trends*; Leszczynski, J., Ed.; World Scientific Publishing, 1995; p 57.

(28) Curtiss, L. A.; Raghavachari, K. In *Computational Thermochemistry*; Irikura, K. K., Frurip, D. J., Eds.; ACS Symposium Series 677; American Chemical Society: Washington, DC, 1998; p 176.

(29) Rinaldi, D.; Rivail, J.-L. *Theor. Chim. Acta* **1973**, *32*, 57.

(30) Tapia, O.; Goscincski, O. *Mol. Phys.* **1975**, *29*, 1653.

(31) Karlström, G. *J. Phys. Chem.* **1988**, *92*, 1318.

(32) Wong, M. W.; Frisch, M. J.; Wiberg, K. B. *J. Am. Chem. Soc.* **1991**, *113*, 4776.

(33) Born, M. *Z. Phys.* **1920**, *1*, 45.

(34) Kirkwood, J. G. *J. Chem. Phys.* **1934**, *2*, 351.

(35) Onsager, L. *J. Am. Chem. Soc.* **1936**, *58*, 1486.

(36) Dillet, V.; Rinaldi, D.; Rivail, J.-L. *J. Phys. Chem.* **1994**, *98*, 5034.

(37) Miertus, S.; Scrocco, E.; Tomasi, J. *Chem. Phys.* **1981**, *55*, 117. Tomasi, J.; Bonnacorsi, R.; Cammi, R.; Valle, F. O. J. *J. Mol. Struct.* **1991**, *234*, 401. Tomasi, J.; Persico, M. *Chem. Rev.* **1994**, *94*, 2027.

(38) Wiberg, K. B.; Rablen, P. R.; Rush, D. J.; Keith, T. A. *J. Am. Chem. Soc.* **1995**, *117*, 4261. Wiberg, K. B.; Keith, T. A.; Frisch, M. J.; Murcko, M. *J. Phys. Chem.* **1995**, *99*, 9072.

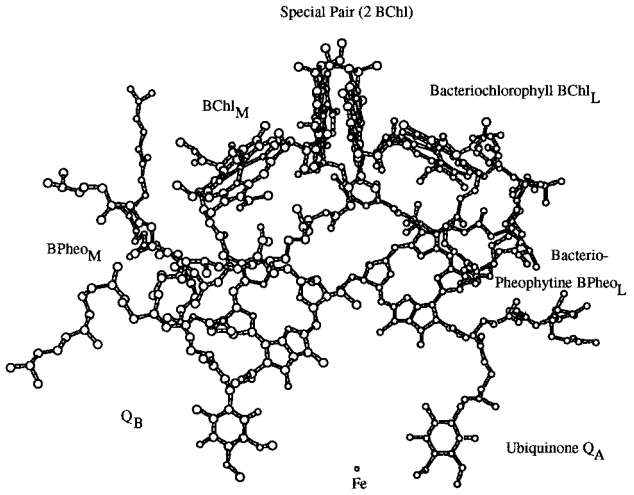

Figure 1. Reaction center in *Rb. sphaeroides*.

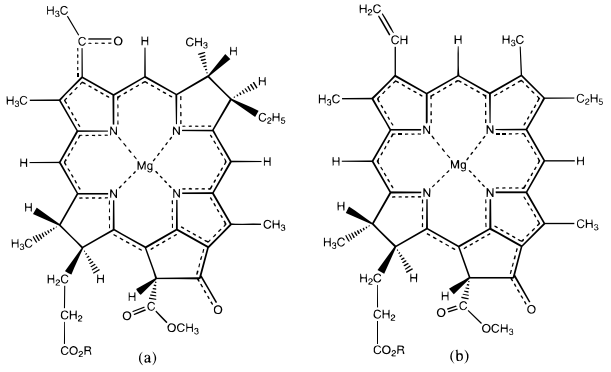

Figure 2. (a) Bacteriochlorophyll *a*, P865, present in *Rb. sphaeroides*. (b) Chlorophyll *a*, P680, present in PSII in plants.

energy to the RC occurs by a sequence of coupled exciton transfers between chlorophyll molecules in the antenna complex. At the reaction center, the light energy initiates a charge-separation process, central for the subsequent photosynthetic reactions. This charge-separation process is studied here for both plants and bacteriosystems, making use of some of the information stored in the X-ray structure of the bacteriosystem.

The photosystem in the purple photosynthetic bacterium *Rhodobacter (Rb.) sphaeroides* is one of the few membrane-bound proteins for which the crystal structure has been determined.[39] The reaction center, shown in Figure 1, consists of two very similar branches, the L and the M branch, of which only the L branch is active in the charge-separation process. Apart from the central dimer of bacteriochlorophyll *a* molecules, P865 (Figure 2a), each branch has an accessory bacteriochlorophyll *a* molecule; a bacteriopheophytin *a* molecule, BPheo, obtained from BChl by replacing the Mg^{2+} ion by two protons; and a ubiquinone (Figure 3a), labeled Q_A in the L branch and Q_B in the M branch. In *Rb. sphaeroides* the photon wavelength of maximal absorption is 865 nm, which corresponds to an energy of 33.0 kcal/mol. The photosynthetic reaction center of another bacterial species, *Rhodopseudomonas (Rps.) viridis*, was the first transmembrane protein to be described in atomic detail,[40] and it is nearly identical to the reaction center of *Rb. sphaeroides*.

The exact structure of the reaction center in photosystem II (PSII) in plants is not known, although progress in this direction

(39) Ermler, U.; Fritzsch, G.; Buchanan, S. K.; Michel, H. *Structure* **1994**, *2*, 925.

(40) Deisenhofer, J.; Epp, O.; Miki, R.; Michel, H. *Nature* **1985**, *318*, 618.

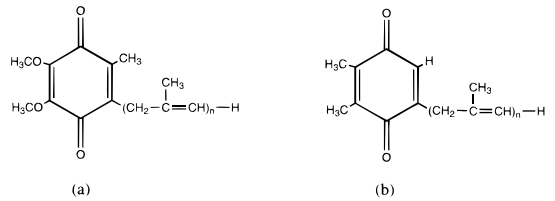

Figure 3. (a) Ubiquinone, the Q_A present in *Rb. sphaeroides*. (b) Plastoquinone, the Q_A present in PSII in plants.

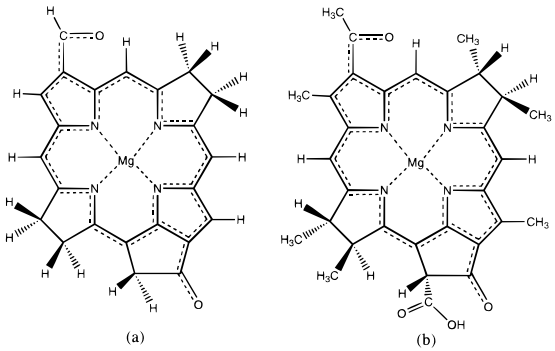

Figure 4. (a) Basic model of bacteriochlorophyll, P865, used in the calculations. (b) Extended model of P865, including models of peripheral groups.

has been reported recently.[7] It is established that this reaction center also consists of two symmetry related branches, one active and one inactive in the charge-separation process. Each branch has at least one chlorophyll *a* molecule, P680 (Figure 2b); a pheophytin *a* molecule, Pheo, which is obtained from Chl by replacing the Mg^{2+} ion with two protons; and a plastoquinone (Figure 3b), labeled Q_A in the active branch and Q_B in the inactive branch. In PSII the photon of maximal absorption has a wavelength of 680 nm corresponding to an energy of 42.0 kcal/mol.

The strategy of the model study described here is to start out by calculating gas-phase results for medium size basic models, shown in Figure 4a for the bacteriosystem. The contributions from the differences between the basic models and larger models more resembling the true systems are then obtained from a set of separate calculations assuming that these effects are additive. Explicit hydrogen-bonding effects and dielectric effects from the surrounding protein are then added until all of the most important effects are expected to be accounted for. In the first subsection III.a. below, the final results from the largest model calculations on the charge-separation processes in the bacteriosystem *Rb. sphaeroides* are discussed, and in the second subsection III.b. the corresponding results for PSII in plants are given. It should already here be noted that the results for PSII by necessity are much more uncertain due to the lack of precise structural information in this case. In subsection III.b. also the next charge-transfer process, the one in which the ionized chlorophyll is reduced by a tyrosine in the neighborhood of the oxygen-evolving manganese center, is discussed. In subsection III.c. the choice of model systems used in the calculations is discussed including a description of the contributions from the different parts of the models to the final results. The reaction energies for the different charge-separation processes are summarized in Table 1 and the individual calculated ionization potentials and electron affinities are summarized in Table 2. It should be noted here that the excited state of the primary donor is never explicitly treated, but it is assumed to be at the energy of the absorbed photon, that is, at 33.0 kcal/mol corresponding to 865 nm.

Table 1. Final Reaction Energies (kcal/mol)

	calcd	exptl
Rb. sphaeroides		
$P865 + Q_A + h\nu \rightarrow P865^+ + Q_A^-$	−22.4	−21.7
$P865 + BPheo + h\nu \rightarrow P865^+ + BPheo^-$	−7.5	−5.8
$P865 + BChl + h\nu \rightarrow P865^+ + BChl^-$	+0.7	−1.1
Photosystem II		
$P680 + Q_A + h\nu \rightarrow P680^+ + Q_A^-$	−20.9	−13.6
$P680 + Pheo + h\nu \rightarrow P680^+ + Pheo^-$	−0.2	
$P680 + Chl + h\nu \rightarrow P680^+ + Chl^-$	−0.3	

Table 2. Calculated Ionization Potentials and Electron Affinities (kcal/mol)

	gas phase	$\epsilon = 4$
Ionization Potentials		
Rb. sphaeroides		
P865	124.3	99.5
photosystem II		
P680	135.6	109.2
Tyr	193.9	153.2
Tyr−His	157.9	127.6
Tyr−His−Glu	149.9	124.2
Tyr−His−Glu−Arg	139.4	119.3
Tyr−His−Glu^-	82.5	102.1
Electron Affinities		
Rb. sphaeroides		
Ubq	49.8	75.8
H_2O−Ubq−H_2O	65.2	86.1
BPheo	47.9	64.9
BPheo−Glu104	53.5	69.2
BChl	42.2	53.9
BChl, H−bonded[a]		58.2
photosystem II		
Psq	46.1	73.3
H_2O−Psq−H_2O	64.9	85.3
Pheo	41.7	58.2
Pheo, H−bonded[a]		62.5
Chl	41.1	55.6
Chl, H-bonded[a]		59.9

[a] Hydrogen-bonding effect taken from BPheo−Glu104.

III.a. The Bacteriosystem *Rb. sphaeroides.* III.a.1. Driving Force for the Charge-Separation Process. The first reaction discussed here is the light-driven charge-separation process in which an electron from the reaction center is transferred to the quinone using the energy of the absorbed photon,

$$P865 + Q_A + h\nu \rightarrow P865^+ + Q_A^- \qquad (1)$$

In *Rb. sphaeroides* the experimental exothermicity for this process is 21.7 kcal/mol.[6,8]

The calculated final ionization potential (IP) including all effects for the bacteriochlorophyll, P865, is 99.5 kcal/mol. To obtain this value, the model bacteriochlorophyll shown in Figure 4a is used, and the effects of peripheral methyl and formyl groups (shown in Figure 4b) and of the axial histidine ligand are added. Also, P865 is known to be a bacteriochlorophyll dimer, the so-called special pair, and the effect on the IP of this dimerization (a decrease of 5.9 kcal/mol) is also included. The details of the calculation of these effects are described in section III.c below. Dielectric effects from the surrounding protein have also been included in this value by using a homogeneous dielectric medium as described in section II. The total effect of the dielectric medium on the ionization potential is a decrease of 24.8 kcal/mol. The total effect on the P865 ionization potential of the molecular extensions of the model shown in Figure 4a is a decrease of 14.1 kcal/mol, which includes changes in dielectric effects.

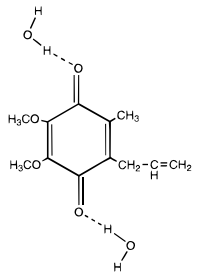

Figure 5. Ubiquinone model used in the calculations, with two hydrogen-bonding water molecules.

To obtain the driving force for the electron transfer from P865 to the quinone Q_A, the electron affinity (EA) of the quinone has to be calculated. The ubiquinone model used in the calculations is shown in Figure 5. The calculated electron affinity of the isolated ubiquinone model, without the two water molecules shown in Figure 5 but with the dielectric effects of the surrounding protein included, is 75.8 kcal/mol. The corresponding gas-phase value is 49.8 kcal/mol. Structural data on the bacterial photosystems indicate that hydrogen bonds between the surrounding protein and the quinones are likely to play a role in the electron-transfer process.[39,41] Such hydrogen bonding cannot be well described by a dielectric continuum and should therefore be explicitly included in the molecular model. In this study water molecules were used to model the amino acids (histidine and alanine) most likely to hydrogen-bond to the Q_A ubiquinone; see Figure 5. With only one hydrogen-bonded water molecule included, the EA is increased from 75.8 to 80.8 kcal/mol (including dielectric effects), and with two water molecules included, the EA becomes 86.1 kcal/mol. The hydrogen bonding is thus quite significant for the EA of the quinones. The reason for this is that the negative charge of the added electron is very localized on the oxygen atoms. Two sets of test calculations were also performed on the simpler benzoquinone, having either two water molecules or two formic acid molecules hydrogen bonded. Very similar effects (differing by only about 2 kcal/mol) on the EA were obtained in the two calculations, showing that the exact nature of the hydrogen bonds is not very important. It is generally considered that the region around the quinones in the reaction center is quite polar and therefore has to be described by a high dielectric constant.[42] In fact, using the small quinone model, without hydrogen bonding, together with $\epsilon = 80$ gives an electron affinity of 85.0 kcal/mol, very close to the value of 86.1 kcal/mol obtained for the model with hydrogen bonding and $\epsilon = 4$. However, a model treating the most important hydrogen bonding explicitly by quantum chemical methods and assigning a uniform low dielectric constant to the rest of the protein is here considered to be most appropriate.

Using the calculated ionization potential of P865 and the electron affinity of the hydrogen-bonded ubiquinone, we can estimate the total driving force for the charge separation in *Rb. sphaeroides* from eq 1. To obtain this energy, it must be remembered that Q_A is sufficiently close to $P865^+$ to experience its positive charge. At a distance of about 30 Å, the screened Coulomb attraction becomes 2.8 kcal/mol, using a simple point charge model ($Q_1Q_2/\epsilon R$). This treatment of the Coulomb attraction is admitedly rather crude, but considering the small

(41) Stowell, M. H. B.; McPhillips, T. M.; Rees, D. C.; Soltis, S. M.; Abresch, E.; Feher, G. *Science* **1997**, *276*, 812.
(42) Warshel, A.; Chu, Z. T.; Parson, W. W. *Science* **1989**, *246*, 112.

size of this effect, it should be accurate enough for the present purpose. Together with the photon energy of 33.0 kcal/mol the driving force becomes 33.0 − 99.5 + 86.1 + 2.8 = 22.4 kcal/mol, in very good agreement with the experimental value of 21.7 kcal/mol; see Table 1. The almost perfect agreement with experiment, however, has to be considered as somewhat fortuitous, since, considering the size of the molecular systems treated, the results of the calculations are expected to have an uncertainty of about 3−5 kcal/mol. In the gas phase, the charge-separation process would be endothermic by 26.1 kcal/mol. The calculated dielectric effects from the surrounding protein on this process are as large as 45.7 kcal/mol.

III.a.2. The Primary Charge-Separation Step. In this section the intermediate role of the pheophytin in the first charge-transfer step is investigated. This electron transfer can be written as

$$\mathrm{P865} + \mathrm{BPheo} + h\nu \rightarrow \mathrm{P865}^{+} + \mathrm{BPheo}^{-} \qquad (2)$$

The chemical model for the pheophytin is chosen in the same way as that for the chlorophyll, with the magnesium ion replaced by two protons. For the bacteriopheophytin in *Rb. sphaeroides* the calculated electron affinity is 69.2 kcal/mol including dielectric effects from the surrounding protein (Table 2). To obtain this value, the same level of modeling as that used for bacteriochlorophyll, shown in Figure 4a, was used and the effects of peripheral methyl and acetyl groups were added (see section III.c). When the effect of the surrounding protein is calculated, the hydrogen bond indicated in the X-ray structure between one keto oxygen in the pheophytin and one glutamic acid (Glu L 104) in one of the peptide chains[39] must be taken into account. Such hydrogen bonding cannot be expected to be well described by a dielectric continuum and has therefore been explicitly included in a set of calculations, showing that the electron affinity of the bacteriopheophytin increases by 4.3 kcal/mol from this interaction when the changes in the dielectric effects from the rest of the protein are taken into account. The surrounding protein effect that is described by the dielectric continuum model contributes an additional 17.0 kcal/mol to the EA of the pheophytin relative to the gas-phase value (Table 2).

The calculated electron affinity of the bacteriopheophytin makes it possible to obtain the energy required for the electron transfer from P865 to the pheophytin. At a distance of 17 Å, the screened Coulomb attraction becomes 4.9 kcal/mol. When the photon energy of 33.0 kcal/mol, is used, these results give an exothermicity for eq 2 of 33.0 − 99.5 + 69.2 + 4.9 = 7.5 kcal/mol. This result agrees very well with an experimental value of 5.8 kcal/mol for the exothermicity of the primary charge-separation step in *Rb sphaeroides*. There are several experimental values for the exothermicity of this step, depending on the time scale.[43] The value chosen here to compare with is the value obtained after 10 ns and should include some molecular relaxation, compatible to the relaxation of the individual molecules included in the present adiabatic values.

III.a.3. The Role of the Accessory Bacteriochlorophyll in *Rb. sphaeroides*. The total driving force for the electron transfer to the quinone Q_A from P865 and the primary step in the charge-separation process, placing the electron on the bacteriopheophytin, are thus found to be in good agreement with experimental estimates. These results give some confidence in the methods used to obtain these values, including the less certain procedure for obtaining the effects of the protein surrounding. It should therefore also be of interest to see what these methods give for the intermediate role of the accessory bacteriochlorophyll. This step can be written as

$$\mathrm{P865} + \mathrm{BChl} + h\nu \rightarrow \mathrm{P865}^{+} + \mathrm{BChl}^{-} \qquad (3)$$

When these calculations were performed, no value had been reported from experimental investigations for this reaction. In fact, it had not even been possible to determine whether the charge separation goes via the accessory bacteriochlorophyll or the electron is transferred directly from P865 to the bacteriopheophytin. After the work described here had been submitted, Hartwich et al.[44] reported fluorescence studies on chemically modified bacterial reaction centers that indicated that the accessory BChl actually is involved as an intermediate and also determined its energetic position to be 1.1 kcal/mol below the excited P865,[44] in good accordance with our calculated value presented below.

The electron affinity of the accessory bacteriochlorophyll in *Rb. sphaeroides* is calculated to be 53.9 kcal/mol, including the effects of the dielectric medium. This can be compared to the value of 64.9 kcal/mol calculated for the bacteriopheophytin before the effects of the hydrogen bonding to the peptide chain are explicitly taken into account. This difference in electron affinity comes mainly from the axial histidine ligand on the bacteriochlorophyll, which decreases the electron affinity by as much as 8.5 kcal/mol. For bacteriopheophytin it was found that the hydrogen-bonding to the surrounding protein plays an important role, and the explicit effect of the bonding to Glu 104 was calculated to increase the electron affinity by 4.3 kcal/mol. In the crystal structure of *Rb. sphaeroides* it is found that at least one water molecule is within hydrogen bonding distance to a keto oxygen in the accessory bacteriochlorophyll in the active L branch. It can therefore be assumed that about the same hydrogen-bonding effect on the electron affinity would be obtained for bacteriochlorophyll as was obtained for the bacteriopheophytin, yielding a final EA of 58.2 kcal/mol for the accessory bacteriochlorophyll. Furthermore, the distance between the accessory bacteriochlorophyll and the special pair is shorter, about 11 Å, as compared to about 17 Å between the bacteriopheophytin and the special pair. This leads to a larger Coulomb attraction in the charge-separated state $\mathrm{P865}^{+}\mathrm{BChl}^{-}$ of 7.6 kcal/mol, compared to 4.9 kcal/mol in the $\mathrm{P865}^{+}\mathrm{BPheo}^{-}$ state. Thus, together with the photon energy of 33.0 kcal/mol and the calculated IP of P865 of 99.5 kcal/mol, these values lead to a weak endothermicity of 33.0 − 99.5 + 58.2 + 7.6 = −0.7 kcal/mol for the charge transfer from P865 to the accessory bacteriochlorophyll according to eq 3. There are two important aspects of this result. First, the value is close to zero, which makes it likely that an electron transfer from the special pair via this accessory bacteriochlorophyll can occur essentially without a barrier. Second, this value shows that the electron transfer from the special pair to the accessory bacteriochlorophyll is less exothermic than the corresponding electron transfer to the bacteriopheophytin (calculated to be exothermic by 7.5 kcal/mol) so that the further electron transfer from the charged accessory bacteriochlorophyll (BChl^{-}) to the bacteriopheophytin would be a downhill process. We therefore conclude that it is energetically feasible that the electron transfer from the special pair to the bacteriopheophytin actually goes via the accessory bacteriochlorophyll. These results for the accessory bacterio-

(43) Woodbury, N. W. T.; Parson, W. W. *Biochim. Biophys. Acta* **1984**, *767*, 345. Woodbury, N. W. T.; Parson, W. W.; Gunner, M. R.; Prince, R. C.; Dutton, P. L. *Biochim. Biophys. Acta* **1986**, *851*, 6. Peloquin, J. M.; Williams, J. C.; Lin, X.; Alden, R. G.; Taguchi, A. K. W.; Allen, J. P.; Woodbury, N. W. *Biochemistry* **1994**, *33*, 8089.

(44) Hartwich, G.; Scheer, H.; Michel-Beyerle, M.-E. Personal communication.

chlorophyll are in line with the results obtained by Warshel and co-workers[13] and also recently by Sim and Makri;[45] see further below.

III.a.4. Comparison to Previous Theoretical Studies. To our knowledge the only quantum chemical calculations performed (as opposed to other types of theoretical studies) on the photosynthetic charge-separation process previously are a few semiempirical calculations treating the primary charge-separation step in the photosynthetic bacterium *Rps. viridis*. For example, Thompson and Zerner[16] have performed INDO calculations on the reaction center of *Rps. viridis* using the X-ray structure and treating all the slightly truncated chlorophylls and pheophytins simultaneously in their gas-phase model. They interpret the excited states of their RC model as different charge-transfer states and obtain a gas-phase energy of 56.4 kcal/mol for the electron transfer from the special pair of bacteriochlorophylls to the bacteriopheophytin. To compare our results to this value, our gas-phase values for the ionization potential of P865 (124.3 kcal/mol) and the electron affinity of BPheo (47.9 kcal/mol) have to be combined with the unscreened Coulomb attraction of 19.6 kcal/mol, yielding a value of 56.8 kcal/mol for the electron transfer from the special pair to the BPheo, very similar to the results of Thompson and Zerner. The similarity between the two results has in fact to be regarded as partly coincidental, taking into account the many differences between the two investigations. Apart from the differences in accuracy of the quantum chemical methods used, there are several other differences. First, Thompson and Zerner use the experimental structure and include no structural relaxation of the chromophores, while we calculate fully optimized adiabatic transitions. Second, their calculation is performed with all chromophores present, while our calculations are done separately on the different chromophores, only taking into account the estimated Coulomb attraction using point charges. Finally, the two sets of results are concerned with different bacterial systems, *Rps. viridis* that contains chromophores of *b* type in their case and *Rb. sphaeroides* that contains chromophores of *a* type in our case.

In a different kind of investigation, Warshel and co-workers[13] extrapolate experimental results for *Rp. viridis* to obtain a gas-phase estimate of 83 kcal/mol for the electron-transfer energy between the separated chromophores, that is, for the primary step in the charge-separation process. They also treat the axial histidine ligand on the chlorophylls as part of the protein, so to compare to their value, our calculated value for the ionization potential of the special pair should be without the effect of the histidine, yielding a gas-phase value of 130.5 kcal/mol. Together with the BPheo gas-phase electron affinity of 47.9 kcal/mol, this leads to a gas-phase value of 82.6 kcal/mol for the electron transfer from the special pair to the bacteriopheophytin at infinite distance from each other, very similar to the value of 83 kcal/mol estimated by Warshel and co-workers for *Rp. viridis*. It should further be noted that for this step in the charge-separation process, good agreement for the final result, which includes the effects of the surrounding protein, is obtained between our present value (7.5 kcal/mol exothermic) and that of Warshel and co-workers (6−7 kcal/mol exothermic[13]). The agreement between both gas-phase and final results implies that the calculated effects of the surrounding protein are very similar in the two procedures.

Several previous theoretical studies have been made with the main purpose being to investigate the effects of the surrounding protein. Gunner et al.[46] have recently made simulation studies on the reaction center of *Rp. viridis* and found that the driving force for the charge-separation process to a large extent should come from a static field generated by charged groups in the surrounding protein. An iron center charged by +2 and a charged arginine residue (Arg L 103) are mainly responsible for this driving force. The total effect from the static field on the electron transfer from the special pair to the pheophytin is found to be as large as 18.4 kcal/mol. In contrast, Warshel, Parson, and co-workers[13] have found that the effects of the heavily screened charges in the protein are very small. In ref 47 calculations were done both on models in which all the ionizable residues were in their neutral states and also on models with all residues other than Glu 104 ionized, and for these two limiting treatments the same energy was obtained for the primary charge-separation step in which the electron is transferred to the pheophytin. In the present study, where such charged groups are not at all included, that is, there is no preferred direction for electron transfer implied by the surrounding, energetics in good agreement with experiments for the electron transfer in *Rb. sphaeroides* from P865 to both the intermediate bacteriopheophytin and the final Q_A are obtained. It should furthermore be noted that if the iron charge would play a large role in the driving force for the electron transfer to the pheophytin, then electrostatics would play an even bigger role for the transfer to the quinone, since this acceptor is closer to iron. If these charge effects actually are important, they imply that there are also other systematic errors of the same size and of opposite sign in the present model results. Even though this seems unlikely, this possibility cannot entirely be ruled out at this stage, and further investigations are necessary to finally settle these issues.

Furthermore, the role of the accessory bacteriochlorophyll has been investigated previously for *Rp. viridis* by several authors.[13,16,45,46,48] In most of these studies[16,46,48] it has been concluded that the accessory bacteriochlorophyll is most likely *not* an intermediate in the charge-separation process. Thompson and Zerner[16] found that the charge-separation step in which the electron moves from the special pair to the accessory BChl should be endothermic by about 15 kcal/mol and concluded that their results argued against an explicit intermediate involving the accessory BChl. Marchi et al.[48] found that the energy associated with moving charge from the special pair to the accessory BChl is far too high (about 15 kcal/mol) and concluded that this finding excludes the possibility of a two-step mechanism within their model for the primary charge transfer. Finally, Gunner et al.[46] calculated the electron-transfer process to the accessory bacteriochlorophyll to be endothermic by about 9 kcal/mol and concluded that this is too high for its formation as a stable intermediate. All three investigations[16,46,48] are based on the gas-phase values for the charge separation obtained in ref 16, which place the reduced BChl state 0.3 kcal/mol above the reduced BPheo state. In the present calculations, the reduced BChl state is calculated to be 5.1 kcal/mol *lower* than the reduced BPheo state in the gas phase. This difference in gas-phase values is likely to contribute to the different conclusion drawn about the role of the accessory BChl by refs 16, 46 and 48 as compared to the present work. On the other hand, Warshel and co-workers[13] obtained the charge-separated

(45) Sim, E.; Makri, N. *J. Phys. Chem. B* **1997**, *101*, 5446.

(46) Gunner, M. R.; Nicholls, A.; Honig, B. *J. Phys. Chem.* **1996**, *100*, 4277.

(47) Alden, R. G.; Parson, W. W.; Chu, Z. T.; Warshel, A. In *The Reaction Center of Photosynthetic Bacteria: Structure and Dynamics*; Michel-Beyerle, M.-E., Ed.; Springer-Verlag: 1996; p 105.

(48) Marchi, M.; Gehlen, M. E.; Chandler, D.; Newton, M. J. *J. Am. Chem. Soc.* **1993**, *115*, 4178.

state that localizes the electron on the accessory bacteriochlorophyll to be only about 3 kcal/mol above the corresponding state with the electron on the pheophytin, which, in turn, was found to be 6−7 kcal/mol below the excited singlet state of the special pair. They concluded that their results are consistent with the formation of a charge-separated state, with the electron on the accessory BChl, as an intermediate in the charge-separation process, although they could not exclude that the reaction proceeds by a superexchange mechanism. The results and conclusions of ref 13 are thus in good agreement with the results in the present investigation. In addition, in a recent quantum dynamics simulation, based on experimental observations on wild-type and modified reaction centers, it was concluded that the optimal parameters determined correspond to a simple two-step electron-transfer mechanism.[45] The optimized value for the position of the reduced accessory BChl was determined to be 1.1 kcal/mol below that of the excited special pair, very close to our value of 0.7 kcal/mol above.

Finally, Zhang and Friesner have performed SCRF calculations at the Hartree−Fock level on models of free bacteriochlorophyll and free bacteriopheophytin.[49] They used models of similar size as in the present work, excluding interactions with the protein, since their goal was to compare to experimental redox potentials measured in the solvent DMF. The gas-phase results for the electron affinities calculated in ref 49 can be compared to the present results, while the dielectric calculations are performed for very different values of ϵ. In ref 49 X-ray structures were used to calculate the gas-phase electron affinity of BPheo to be 29.9 kcal/mol and that of BChl to be 32.6 kcal/mol. The corresponding values obtained for the optimized structures in the present work are 47.9 and 50.7 kcal/mol, respectively. To arrive at this BChl value, in the present work the lowering effect of the axial histidine (−8.5 kcal/mol) has been subtracted. The main source of the difference between the two sets of results is the lack of electron correlation effects in the Hartree−Fock calculations in ref 49. Electron correlation, included in the present density-functional calculations, is expected to increase the electron affinity. Of minor importance for the differences in the results, probably, is the fact that BChl and BPheo *b* are modeled in ref 49, while BChl and BPheo *a* are modeled in the present work. It is, however, interesting to note that the difference in electron affinity between the BPheo and the BChl is very similar in the two calculations, 2.7 kcal/mol in ref 49 and 2.8 kcal/mol in the present work.

III.b. Photosystem II (PSII) in Plants. As mentioned above, the exact structure of the reaction center in photosystem II (PSII) in plants is not known, and it is therefore much more difficult to choose the most appropriate models for calculation. The purpose of this section is to apply similar models and computational techniques to photosystem II as were found above to give agreement with experiment for the charge-separation process in the bacteriosystem. In the first subsection below the energies of the electron-transfer process from the reaction center chlorophyll molecule to the quinone Q_A driven by the photon energy stored in an excited state of the chlorophyll, are discussed. Calculated ionization energies and electron affinities of the chlorophylls and the quinones involved are reported. In the second subsection the primary charge-separation step, where the electron is transferred from the reaction center chlorophyll to a pheophytin molecule placed between the chlorophyll and the quinone, is discussed. In a third subsection the process involved in the transfer of the energy from $P680^+$ to the active tyrosine in the neighborhood of the manganese cluster is considered. This step also involves the release of the proton created in this process, via a histidine residue, toward the exterior of the thylakoid membrane.

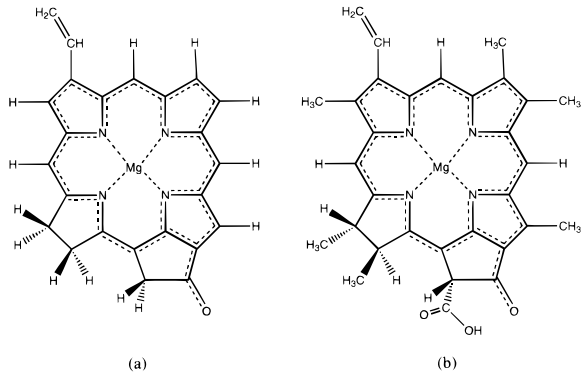

Figure 6. (a) Basic model of chlorophyll, P680, used in the calculations. (b) Extended model of P680, including methyl and formyl groups.

III.b.1. Driving Force for the Charge-Separation Process. In this section the exothermicity is calculated for the light-driven charge-separation process written as

$$P680 + Q_A + h\nu \rightarrow P680^+ + Q_A^- \qquad (4)$$

In PSII this process is known from experiment to be exothermic by 13.6 kcal/mol.[2,6] The driving force is thus 8.1 kcal/mol smaller for PSII than for the bacteriosystem, which has an experimental driving force of 21.7 kcal/mol as discussed above.

The calculated ionization potential (IP) of the chlorophyll P680 is 109.2 kcal/mol, which is almost 10 kcal/mol larger than for the bacteriochlorophyll P865 that has an IP of 99.5 kcal/mol. To obtain the P680 ionization potential, the model chlorophyll shown in Figure 6a was used and the effects of the peripheral substituents (see Figure 6b) and the axial histidine were added. The details of the calculations of the added effects are described in section III.c below. The P680 models in Figure 6 correspond to the models of the bacteriochlorophyll P865 shown in Figure 4. No dimerization effect is included for P680, since spectroscopic results indicate that if there is a chlorophyll dimer in PSII the two molecules are much more weakly interacting than in the bacterial reaction center.[6,9,50] Therefore, the dimerization effect should be smaller than that for the bacteriosystem, which is here calculated to be 5.9 kcal/mol. Dielectric effects from the surrounding protein were included in the same way as for the bacteriosystem, that is, by using a homogeneous dielectric medium. The total effect of the dielectric medium on the ionization potential is a decrease of 26.4 kcal/mol, and the total effect of the model extensions is 10.8 kcal/mol, with changes in dielectric effects included.

The plastoquinone model used in the calculations is chosen in the same way as the ubiquinone model was that is, all the features of the true quinone are retained, except that the long isoprenoid tail is replaced by a propenyl unit; see Figure 7. The calculated electron affinity for this plastoquinone model, with dielectric effects of the surrounding protein included, is 73.3 kcal/mol, and the corresponding gas-phase value is 46.1 kcal/mol. A recent quantum chemical analysis of the experimental EPR spectra suggests that there are two hydrogen bonds on the Q_A in PSII,[51] which is similar to the bacteriosystem. As in the

(49) Zhang, L.; Friesner, R. A. *J. Phys. Chem.* **1995**, *99*, 16479.

(50) Svensson, B.; Etchebest, C.; Tuffery, P.; VanKan, P.; Smith, J.; Styring, S. *Biochemistry* **1996**, *35*, 14486.

(51) Eriksson, L. A.; Hihmo, F.; Siegbahn, P. E. M.; Babcock, G. T. *J. Phys. Chem.* **1997**, *101*, 9496.

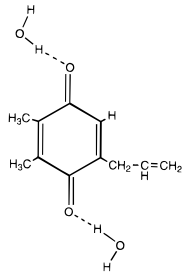

Figure 7. Plastoquinone model used in the calculations, with two hydrogen-bonding water molecules.

bacteriosystem, water molecules were used to model the hydrogen bonds, and the calculated electron affinity of plastoquinone with two hydrogen-bonded water molecules, is 85.3 kcal/mol, which includes a dielectric effect of 23.4 kcal/mol, see Figure 7. With only one water molecule hydrogen bonded, the electron affinity is found to be 79.1 kcal/mol, when dielectric effects are included.

When the calculated ionization potential of P680 and the electron affinity of the plastoquinone are used, including two hydrogen bonds, an estimate of the total driving force for electron transfer in PSII can be obtained from eq 4. Since the distance between P680 and Q_A is not known in PSII, the value for the Coulomb attraction is taken to be the same as in the bacteriosystem, 2.8 kcal/mol. Together with the photon energy of 42.0 kcal/mol, this leads to a driving force of 42.0 − 109.2 + 85.3 + 2.8 = 20.9 kcal/mol, somewhat larger than the experimental value of 13.6 kcal/mol. In the gas phase, this charge separation is calculated to be endothermic by 31.7 kcal/mol. The total dielectric effect is calculated to be 49.8 kcal/mol.

The error of 7.3 kcal/mol in the calculated driving force for the charge separation in PSII is acceptable considering the uncertainties in the structure of the reaction center. As discussed above, the corresponding error in the bacteriosystem is much smaller, only 0.6 kcal/mol. This means that the difference in driving force between the two systems is not very well reproduced. The driving force for PSII is calculated to be only 1.5 kcal/mol smaller than for the bacteriosystem, and the experimental difference in driving force for the two photosystems is 8.1 kcal/mol. Several error sources are conceivable, including the possibility that "P680" actually refers to the entire collection of pigments in the PSII reaction center,[9] but the lack of exact structural information for PSII is probably the main reason for the discrepancy.

III.b.2. The Primary Charge-Separation Step. The first step in the electron-transfer process in PSII can be written as

$$\mathrm{P680} + \mathrm{Pheo} + h\nu \rightarrow \mathrm{P680^+} + \mathrm{Pheo^-} \qquad (5)$$

For the pheophytin in PSII, an electron affinity of 58.2 kcal/mol is calculated by using a model corresponding to the P680 model in Figure 6b, with the magnesium ion replaced by two protons and dielectric effects included. The dielectric effect obtained for this system is 16.5 kcal/mol. It is not yet known whether hydrogen bonding to the pheophytins in PSII is present, but this is quite likely, and a hydrogen-bonding effect of 4.3 kcal/mol, taken from the bacteriosystem, is therefore added to the electron affinity of the PSII pheophytin, yielding a final value of 62.5 kcal/mol.

To calculate the energy required for the electron transfer from P680 to the pheophytin, it is necessary to include the Coulomb attraction between $Pheo^-$ and $P680^+$. Since the distance between the pheophytin and P680 in PSII is not known, the value for the screened Coulomb attraction is taken from the bacteriosystem to be 4.9 kcal/mol. Together with the photon energy of 42.0 kcal/mol, these results indicate that the electron transfer to the pheophytin, following eq 5, is close to thermoneutral; 42.0 − 109.2 + 62.5 + 4.9 = 0.2 kcal/mol. There is no experimental value for the energetics of this reaction step. However, even if this process has mostly been assumed to be slightly exothermic, some recent time-resolved absorption and fluorescence results have been interpreted to indicate that the primary charge-separation step in PSII is slightly endothermic (see refs 10 and 11 and references therein). In the bacteriosystem the primary charge-separation step is calculated to be exothermic by 7.5 kcal/mol, slightly larger than the experimental estimate of 5.8 kcal/mol. The difference between the bacteriosystem and PSII is thus a 7.3 kcal/mol larger exothermicity for the bacteriosystem, which is in agreement with the experimental data that indicate that this step should be less stabilized for photosystem II than for the bacteriosystem.

III.b.3. The Creation of the Tyrosyl Radical in PSII. Once the charge separation has taken place by the sequence of events described above, the next step is to transfer these charges further to other places where additional reactions will occur. The negative charge on the quinone Q_A is first transferred to another quinone, Q_B, where it will be eventually be combined with protons to form a QH_2 molecule. This molecule has no charge and essentially also lacks a dipole moment and can therefore travel almost freely across the thylakoid membrane. The fate of the electrons after the charge separation will not be discussed further here. Instead, the focus of interest in the present subsection is the re-reduction of the ionized chlorophyll, $P680^+$, which occurs through the oxidation of a tyrosine residue situated in the region of the manganese center in PSII. An important aspect of all secondary processes where charge is transferred is that there should be only a very small driving force, in order not to waste energy unnecessarily.[2,52] This is quite different from the primary charge-separation process where a relatively large driving force is needed to prevent an undesirably rapid charge recombination.

In the neighborhood of P680, the residues with the lowest redox potentials are tyrosines. There is one tyrosine, Tyr_Z (Tyr 161 of the D1 polypeptide), close to the manganese center that is oxidized during the water-splitting reactions. This Tyr_Z has been shown to be the only electron carrier between P680 and the Mn cluster.[6,53,54] Thus, $P680^+$ is re-reduced by Tyr_Z, which in turn is re-reduced by the water-coordinated Mn complex. To prevent charge-recombination reactions between $P680^+$ and Q_A^-, the re-reduction of $P680^+$, that is, the electron transfer from Tyr_Z to $P680^+$, has to be a very fast process (nanosecond). To describe the energetics of this electron-transfer process is the main goal in the present subsection. Also, after the charge-transfer Tyr_Z is observed as a neutral radical,[55] not a positively charged one, which also needs to be explained.

The property relevant for the electron transfer to $P680^+$ is the ionization potential (IP) of tyrosine. The calculated gas-phase IP of phenol, which is used as a model for tyrosine, is 193.9 kcal/mol. The experimental value is 196.2 kcal/mol. The gas-phase IP of tyrosine is thus much larger than the corre-

(52) Hoganson, C. W.; Babcock, G. T. *Science* **1997**, *277*, 1953.
(53) Britt, R. D In *Oxygenic Photosynthesis: The Light Reactions*; Ort, D. R., Yocum, C. F., Eds.; Kluwer: Dordrecht, The Netherlands, 1996; p 137.
(54) Babcock, G. T.; Barry, B. A.; Debus, R. J.; Hoganson, C. W.; Atamion, M.; McIntosh, L.; Sitole, I.; Yocum, C. F. *Biochemistry* **1989**, *28*, 9557.
(55) Barry, B. A.; Babcock, G. T. *Proc. Natl. Acad. Sci. U.S.A.* **1987**, *84*, 7099.

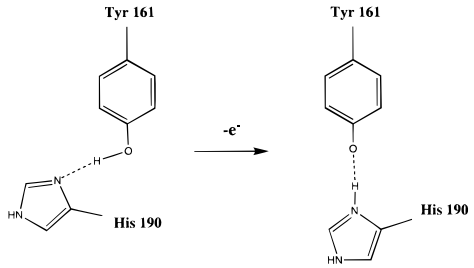

Figure 8. Ionization of the Tyr−His pair.

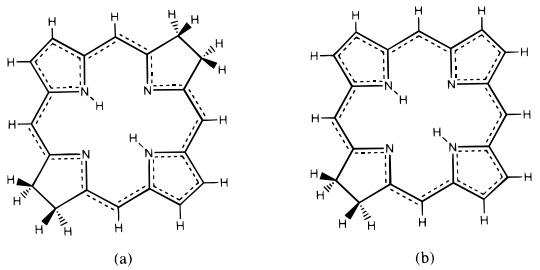

Figure 9. Simplest models used for (a) H_2−bacteriochlorin and (b) H_2−chlorin.

sponding IP of 135.6 kcal/mol for P680. In the gas phase, no charge transfer from $P680^+$ to tyrosine would therefore take place. The polarization of the protein is one of two important factors for the charge transfer. The dielectric effects lower the IP of tyrosine by 40.7 kcal/mol, to 153.2 kcal/mol, while they lower the IP of P680 by only 26.4 kcal/mol, to 109.2 kcal/mol. The reason for this difference in dielectric effect is simply that the tyrosine is smaller than the chlorophyll.

The second important factor allowing for the charge transfer from $P680^+$ to tyrosine is the presence of a hydrogen-bonding histidine. Tyr_Z (Tyr 161) is known to be hydrogen bonded to His 190 (ref 2 and references therein). The calculated result for the IP of the tyrosine−histidine pair (Figure 8), modeled by phenol−imidazole, is 127.6 kcal/mol including dielectric effects. The presence of the histidine has thus lowered the IP by 25.6 kcal/mol, bringing it closer to the region of the IP for P680. The reason for this large effect is that a proton is transferred from tyrosine to the more basic histidine. The IP of 127.6 kcal/mol is thus an adiabatic IP, the vertical one being about 15 kcal/mol higher.

The adiabatic ionization of the tyrosine−histidine pair thus moves a proton from tyrosine to histidine. This result explains the fact that only neutral tyrosyl radicals have been identified in PSII. This is important for the oxygen-evolving process where the neutral tyrosyl radical is postulated to abstract hydrogen atoms, both protons and electrons, from water molecules bound as manganese ligands.[2,52,53,56−59]

The process of moving the electron from Tyr_Z to $P680^+$ should be thermoneutral or slightly exothermic.[6] The IP of 127.6 kcal/mol for the tyrosine−histidine pair is still quite far from allowing this electron transfer, since the calculated IP for P680 is 109.2 kcal/mol. Therefore, some important aspects of the Tyr_Z's surroundings are still missing in this chemical model. In a first attempt to improve the model the next members of the hydrogen-bonded chain were included in the calculations to stabilize the protonated histidine. For Tyr_Z the next member in the hydrogen-bonded chain is probably a glutamic acid[60] (see also discussion in ref 2) here modeled by a formic acid, which reduces the tyrosine IP further but only by 3.4 kcal/mol. This is not a very surprising result, since it would be expected that a base, rather than an acid, is required to stabilize the protonation of the histidine residue. For this reason, an arginine, modeled by formamidine hydrogen bonded to the glutamic acid, was added. The arginine reduces the IP by another 4.9 kcal/mol. The IP for the Tyr-His-Glu-Arg sequence is thus found to be 119.3 kcal/mol, including dielectric effects, which is still 10.1 kcal/mol larger than the IP of 109.2 kcal/mol for P680. It is clear from these results that the IP of tyrosine is strongly dependent on the immediate surroundings and, in particular, the tyrosine IP is decreasing with increasing basicity of the hydrogen-bonded chain. It is also clear that the models used in the calculations are not converged with respect to this property, and it is increasingly apparent that the lack of structural information is quite critical for the modeling problem. Rather than continuing to guess at the precise surrounding of Tyr_Z, a more drastic model was made in order to obtain an idea of the boundary conditions involved in this process. As an extreme model, a negatively charged glutamate ion (modeled by a formate ion) was therefore added to the chain, yielding the Tyr-His-Glu^- chain. The IP for this system is found to be 102.1 kcal/mol, including dielectric effects. This model is also interesting, since it gives the lowest reorganization barrier (about 10 kcal/mol, as compared to 25−30 kcal/mol for the other models) to change the initial state into the optimal structure of the ionized system. As mentioned above, the ionization is a fast process, in the nanosecond region, which means that there must be only small energies involved in the transformation between the structures of the initial and the ionized states. However, as a consequence of the total charge of this model, it is not considered as a realistic description of the peptide chain, but it shows that it is possible to decrease the tyrosine IP even below the value of 107−109 kcal/mol needed to make the electron transfer to $P680^+$ thermoneutral or slightly exothermic. More realistic neutral models for the Tyr_Z environment are now under investigation. In this context it should also be noted that the IP of Tyr_Z is expected to be affected by the coupling to the manganese−water complex.

III.c. Model Effects on the Chromophore Energetics. In this section the procedures used to determine the ionization potentials and electron affinities of the chlorophyll and pheophytin molecules are described. The calculations are performed in such a way that the complexity of the models is increased stepwise. The motivation and background to this approach is two-fold. First, it is important to keep the models as small as possible, to minimize the computer resources required, and second, extra chemical insights can be gained by studying the effects of different changes in the models used.

III.c.1. Basic Model. In a first attempt to keep the size of the models used at a minimum, chlorin was used as a model for P680 (Mg−chlorin) and Pheo (H_2−chlorin) and bacteriochlorin was used as a model for P865 (Mg−bacteriochlorin) and BPheo (H_2−bacteriochlorin); see Figure 9. At this level of modeling, the calculated ionization potentials, including dielectric effects of the surrounding protein, are 103.2 kcal/mol for bacteriochlorophyll, P865, and 115.3 kcal/mol for chlorophyll, P680. It can also be noted that the ionization potential of Mg−porphyrin is calculated to be 125.5 kcal/mol, and the decrease of the IP for each pyrrole ring that becomes

(56) Blomberg, M. R. A.; Siegbahn, P. E. M.; Styring, S.; Babcock, G.T.; Åkermark, B.; Korall, P. *J. Am. Chem. Soc.* **1997**, *119*, 8285.
(57) Coudle, M. T.; Pecoraro, V. L. *J. Am. Chem. Soc.* **1997**, *119*, 3415.
(58) Tommos, C.; Tang, X.-S.; Warncke, K.; Hoganson, C. W.; Styring, S.; McCracken, J.; Diner, B. A.; Babcock, G. T. *J. Am. Chem. Soc.* **1995**, *117*, 10325.
(59) Gilchrist, M. L.; Ball, J. A.; Randall, D. W.; Britt, R. D. *Proc. Natl. Acad. Sci. U.S.A.* **1995**, *91*, 9545.
(60) Chu, H.-A.; Nguyen, A. P.; Debus, R. J. *Biochemistry* **1995**, *34*, 5839.

partially reduced is thus 10−12 kcal/mol. Using these ionization potentials together with the photon energies, the electron affinities for the quinone, Q_A, for each system, and the screened Coulomb attraction from the bacteriosystem of 2.8 kcal/mol, the driving force for the charge-separation process can be calculated. For the bacteriosystem, a driving force of 33.0 − 103.2 + 86.1 + 2.8 kcal/mol = 18.7 kcal/mol is obtained, and for PSII a value of 42.0 − 115.3 + 85.3 + 2.8 = 14.8 kcal/mol is obtained. These values are in good agreement with the experimental estimates of the driving forces, 21.7 and 13.6 kcal/mol, respectively. At an early stage of this study it was therefore concluded that this level of modeling for the chlorophyll type molecules was sufficient. However, when the primary step of the charge separation was studied, the conclusion was quite different.

The calculated electron affinity for BPheo, including dielectric effects, using H_2−bacteriochlorin as a model, is 49.0 kcal/mol, and that of Pheo, using H_2−chlorin as a model, is 49.2 kcal/mol. The corresponding H_2−porphyrin has an electron affinity of 49.9 kcal/mol, and it can be concluded that the electron affinities are much less sensitive to the reduction of the pyrrole rings than are the ionization potentials. Using these electron affinities for the pheophytins, the chlorophyll ionization potential reported in the preceding paragraph, and the screened Coulomb attraction of 4.9 kcal/mol taken from the bacteriosystem, we can calculate the energetics of the primary charge-separation step. For the bacteriosystem, the reaction energy is 33.0 − 103.2 + 49.0 + 4.9 = −16.3 kcal/mol, that is, this step is strongly endothermic, in clear contradiction to the experimental observation that this step should be exothermic by 5.8 kcal/mol. For PSII, the primary charge-separation step at this level of modeling is also found to be strongly endothermic, 42.0 − 115.3 + 49.2 + 4.9 = −19.2 kcal/mol. Thus, for this reaction step, the level of modeling depicted in Figure 9 leads to errors of about 20 kcal/mol for both the bacteriosystem and PSII.

At this stage, it was suspected that the keto groups that are part of the aromatic system could be important for the electron affinity of the pheophytins, and these were therefore also included, leading to the level of modeling shown for the corresponding chlorophyll molecules in Figure 4a and 6a. Use of the model of Figure 4a for BPheo indeed leads to an increase of the calculated electron affinity of 18.8 kcal/mol, yielding a value of 67.8 kcal/mol. Such an increase in the pheophytin electron affinities would lead to a decrease in the calculated endothermicity of the primary charge-separation step of almost the same amount as the error obtained in the preceding paragraph, thus pointing toward a good agreement with the experimental situation if this level of modeling is used instead. However, if the modeling shown in Figure 4a is also used for the chlorophyll molecules, it turns out that the ionization potentials are also changed. The ionization potential of P865 is increased by 10.4 kcal/mol, yielding a value of 113.6 kcal/mol, partly canceling the effect on the primary step from the increased electron affinity of the pheophytin. Thus, the calculated energetics using this new model are not in as good agreement with experiment as first expected, and several other improvements of the model were therefore investigated as described below.

III.c.2. Peripheral Substituents. In a paper by Ghosh,[61] where substituent effects on the ionization potential of H_2−porphyrin were studied, it was shown that the fully methyl-substituted species has an ionization potential that is as much as 13 kcal/mol lower than that of the unsubstituted one. It was therefore expected that the models shown in Figures 4a and 6a might suffer from the replacement of the different peripheral groups in the true system (Figure 2) by H atoms. Thus, we decided to investigate the effect on ionization potentials and electron affinities of using methyl groups to model the peripheral groups, and thus, the models in Figure 4b and 6b were introduced, where also a formyl group is used to model an acetyl group. Also, for these models the geometries were fully optimized for both the neutral and charged systems. Dielectric effects were calculated for every system. In this way it was found that the peripheral groups introduced in the model of Figure 4b decrease the ionization potential of P865 by 4.6 kcal/mol as compared to the basic model of Figure 4a, when also the changes in dielectric effects are taken into account. The gas-phase effect of the peripheral groups is somewhat larger, a decrease in the ionization potential of 5.8 kcal/mol. The corresponding value for BPheo is a decrease in the electron affinity of 2.9 kcal/mol. In this case, the same effect is obtained in the gas phase. The effect on the electron affinity of the accessory BChl is a decrease of 4.0 kcal/mol, including dielectric effects, and the corresponding gas-phase value is only 0.9 kcal/mol. For PSII the effect of the peripheral groups is calculated from the differences between the models in Figure 6. Thus, the ionization potential of P680 decreases by 4.7 kcal/mol and the effect on the electron affinity of Pheo is a decrease of 1.8 kcal/mol, both values including changes in dielectric effects. In the gas phase, the effect on the ionization potential is a decrease of 6.2 kcal/mol and on the electron affinity a decrease of 1.3 kcal/mol. It is thus found that for the Mg−chlorophylls the peripheral substituents have smaller effects on the ionization potential (about 6 kcal/mol in the gas phase) than for the case of H_2−porphyrin (13 kcal/mol), studied in ref 61 and mentioned above. For the electron affinity of the H_2−chlorophylls, the peripheral substituents have an even smaller effect (1−3 kcal/mol in the gas phase).

III.c.3. Axial Histidine Ligand on the Chlorophylls. For the special pair bacteriochlorophylls, and also for the accessory chlorophylls in the bacteriosystem, the central Mg atom is coordinated to a histidine residue in the surrounding protein. As a result of a comparison of the amino acid sequences in PSII and in the bacteriosystem, it has been concluded that the P680 chlorophyll(s) in PSII have axial histidine ligands such as the special pair in the bacteriosystem, while the accessory chlorophylls in PSII do not have such ligands. The effect on the ionization potential of the chlorophylls of this coordination can hardly be described by the dielectric continuum model of the protein, and an explicit imidazole ligand of the Mg atom of the chlorophylls is therefore introduced. The chlorophyll model used to calculate this effect is shown in Figure 4a for the bacteriosystem and in Figure 6a for PSII. In all cases the structures are optimized, and in Figure 10 the resulting ionized P865 structure including the imidazole ligand is shown. For the bacteriochlorophyll, P865, the effect of this axial ligand is a decrease of the ionization potential of 3.6 kcal/mol, when changes in dielectric effects are taken into account, and for the accessory bacteriochlorophyll the electron affinity decreases by 8.4 kcal/mol. In the gas phase the effect is a decrease in the ionization potential of 6.2 kcal/mol and a decrease in the electron affinity of 7.0 kcal/mol. For P680 the corresponding values are 6.1 kcal/mol, including dielectric effects, and 8.5 kcal/mol in the gas phase. For P680 a final value for the ionization potential of 109.2 kcal/mol is obtained when the effects of the axial histidine ligand and the peripheral groups are included. The total effect added in this way is 10.8 kcal/mol, including

(61) Ghosh, A. *J. Am. Chem. Soc.* **1995**, *117*, 4691.

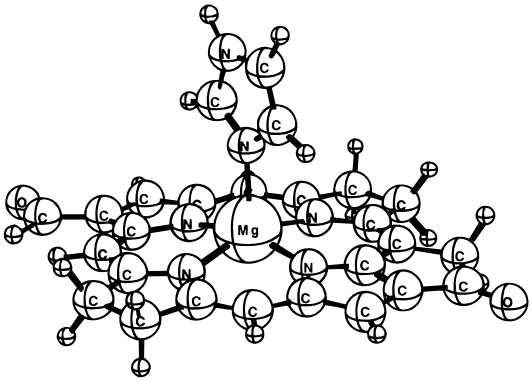

Figure 10. Model used to calculate the effect of the histidine ligand on P865, optimized structure for the ionized system.

dielectric effects and assuming additivity of the different model effects.

For the accessory chlorophyll in the bacteriosystem the axial histidine ligand was calculated to decrease the electron affinity by as much as 8.5 kcal/mol. This is the main source of the calculated difference in driving force for the charge separation to the accessory bacteriochlorophyll and that to the pheophytin in the bacteriosystem. It is interesting to note that the amino acid sequences indicate that there are no axial histidines ligating to the accessory chlorophylls in photosystem II.[6] From the results presented above, by the placement of the reduced accessory chlorophyll in PSII at about the same level as the excited P680 (see Tables 1 and 2 above), it can be expected that if there were such axial histidine ligands present, this would give rise to unsurmountable barriers for a charge-separation process via the accessory chlorophyll in PSII. In the calculations of the energetics for the charge separation to the accessory chlorophyll in PSII, the hydrogen-bonding and Coulomb attraction were taken from the bacteriosystem.

III.c.4. Special Pair in the Bacteriosystem. In the bacteriosystem, the reaction center pigment complex that is excited by energy transfer from the antenna system is a dimer of two almost parallel identical BChl *a* molecules; see Figure 1. The effect of dimerization on the ionization potential is calculated by using the X-ray structure without further geometry optimization and truncating the two BChls to correspond to the model in Figure 4, as shown in Figure 11. After the changes in dielectric effects are taken into account the ionization potential of P865 decreases by 5.9 kcal/mol from the dimerization. The gas-phase value shows a decrease of 8.7 kcal/mol. For P865 this leads to a final value for the ionization potential of 99.5 kcal/mol, assuming additivity of the dimerization, histidine, and peripheral group effects. All three effects go in the same direction, decreasing the ionization potential by altogether 14.1 kcal/mol when dielectric effects are included. As mentioned above, there are indications that the corresponding chlorophyll molecules in PSII interact much more weakly than in the bacteriosystem, and therefore no dimerization effect is included in the IP of P680.

III.c.5. Hydrogen Bonding to the Pheophytins. As noted above, the crystal structure of the bacteriosystem clearly indicates the presence of hydrogen bonding between BPheo and a glutamic acid residue (Glu L 104) in the surrounding protein.[39] The effect on the electron affinity is calculated by using the Figure 4a level of model for BPheo and a formic acid model of the glutamic acid; see Figure 12. The structures are optimized for both the neutral and the charged system. An increase in the electron affinity for BPheo of 4.3 kcal/mol is obtained after

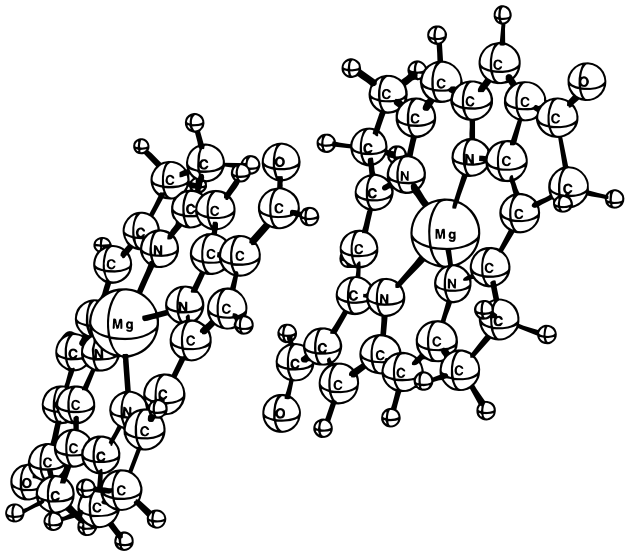

Figure 11. Model used to calculate the special pair effect in the bacteriosystem, experimental structure.

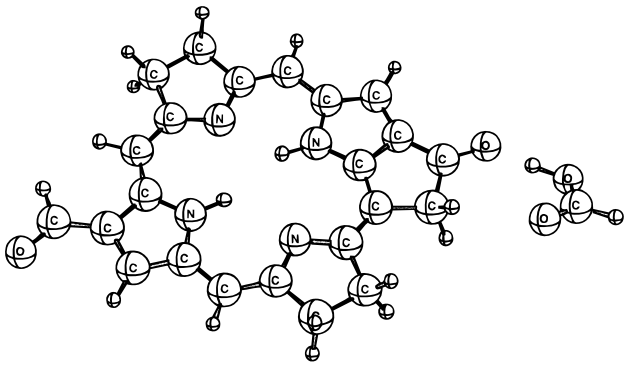

Figure 12. Model used to calculate the hydrogen-bonding effect on the electron affinity of bacteriopheophytin, optimized structure for the charged species.

the changes in dielectric effects are taken into account. The gas-phase effect is an increase of 5.6 kcal/mol. Together with the peripheral substituent effect of −2.9 kcal/mol described above, this leads to a final electron affinity for the BPheo of 69.2 kcal/mol, including dielectric effects. It is interesting to note that a decrease in the electron affinity of BPheo of about 4 kcal/mol, which would occur if the hydrogen bonding possibility were omitted, is not expected to hinder the charge-separation process, since reaction 2 would still be exothermic. This result is in agreement with the results from mutagenesis experiments, showing only a slight decrease in charge-transfer rates when the hydrogen-bonding Glu L 104 is replaced by less strongly hydrogen-bonding residues, such as Gln and Leu.[62]

IV. Conclusions

Our computational results for the bacterial reaction center show good agreement with the experimentally observed charge separation energetics. They highlight the role of the local protein environment in tuning the properties of the various chromophores for specific function and provide support for an energetically accessible charge-separated state that involves the

(62) Bylina, E. J.; Kirmaier, C.; McDowell, L.; Holten, D.; Youvan, D. C. *Nature* **1988**, *336*, 182.

monomer BChl. In PSII, the lack of a well-defined structure softens the conclusions that we are able to draw to some extent. Nonetheless, three important insights emerge. First, the charge separation to produce the $P680^+Pheo^-$ state is much less strongly driven, which is consistent with recent experimental work on the initial photochemistry in the reaction center.[8−11] Second, the absence of axial histidine ligation to the accessory Chl appears necessary to facilitate formation of the $P680^+Pheo^-$ state. This observation provides a basis for rationalizing the puzzling difference in axial ligation for the monomer chromophore in PSII relative to the bacterial system. Finally, the importance of both electron and proton transfers to the energetics of the

$$P680^+ Y_Z \rightarrow P680Y_Z\cdot + H^+$$

reaction emerges and highlights recent work that indicates that failure to remove the proton efficiently during Y_Z oxidation drastically impairs electron donation to $P680^+$.[60,63,64] see also references 52, 53, and 2.

JA9805268

(63) Nixon, P. J.; Diner, B. A. *Biochem. Soc. Trans.* **1994**, *22*, 338.
(64) Hays, A.-M. A.; Vassiliev, I. R.; Golbeck, J. H.; Debus, R. J. Submitted.